Published in final edited form as:

Neuroscience. 2016 June 21; 326: 84–94. doi:10.1016/j.neuroscience.2016.03.054.

Unilateral Microinjection of Acrolein into Thoracic Spinal Cord Produces Acute and Chronic Injury and Functional Deficits

Alexander Gianaris[1,#], **Nai-Kui Liu**[1,#], **Xiao-Fei Wang**[1], **Eddie Oakes**[1], **John Brenia**[1], **Thomas Gianaris**[1], **Yiwen Ruan**[1], **Ling-Xiao Deng**[1], **Maria Goetz**[1], **Sasha Vega-Alvarez**, **Qing-Bo Lu**[1], **Riyi Shi**[2,*], and **Xiao-Ming Xu**[1,*]

Alexander Gianaris: redgianaris@gmail.com; Nai-Kui Liu: nailiu@iupui.edu; Xiao-Fei Wang: ntwxf001@163.com; Eddie Oakes: racer12b@gmail.com; John Brenia: jbrenia@iupui.edu; Thomas Gianaris: tgianari@iupui.edu; Yiwen Ruan: yiwenruan@yahoo.com; Ling-Xiao Deng: dengl@iupui.edu; Maria Goetz: mariagoetz1@gmail.com; Sasha Vega-Alvarez: saschavega@gmail.com; Qing-Bo Lu: qilu@iupui.edu; Riyi Shi: shir@purdue.edu; Xiao-Ming Xu: xu26@iupui.edu

[1]Spinal Cord and Brain Injury Research Group, Stark Neurosciences Research Institute Department of Neurological Surgery & Goodman Campbell Brain and Spine, Indiana University School of Medicine, Indianapolis, IN 46202

[2]Department of Basic Medical Sciences, College of Veterinary Medicine and Weldon School of Biomedical Engineering, Purdue University, West Lafayette, IN 47907

Abstract

Although lipid peroxidation has long been associated with spinal cord injury (SCI), the specific role of lipid peroxidation-derived byproducts such as acrolein in mediating damage remains to be fully understood. Acrolein, an α-β unsaturated aldehyde, is highly reactive with proteins, DNA, and phospholipids and is considered as a second toxic messenger that disseminates and augments initial free radical events. Previously, we showed that acrolein increased following traumatic SCI and injection of acrolein induced tissue damage. Here, we demonstrate that microinjection of acrolein into the thoracic spinal cord of adult rats resulted in dose-dependent tissue damage and functional deficits. At 24 hours (acute) after the microinjection, tissue damage, motoneuron loss, and spinal cord swelling were observed on sections stained with cresyl violet. Luxol fast blue staining further showed that acrolein injection resulted in dose-dependent demyelination. At 8 weeks (chronic) after the microinjection, cord shrinkage, astrocyte activation, and macrophage infiltration were observed along with tissue damage, neuron loss, and demyelination. These pathological changes resulted in behavioral impairments as measured by both the Basso, Beattie, and Bresnahan (BBB) locomotor rating scale and grid walking analysis. Electron microscopy further demonstrated that acrolein induced axonal degeneration, demyelination, and macrophage

[*]Corresponding author: Xiao-Ming Xu, M.D., Ph.D., Professor and Scientific Director, Spinal Cord and Brain Injury Research Group, Stark Neurosciences Research Institute, Department of Neurological Surgery, Indiana University School of Medicine, 950 W Walnut St, R-2 Building, Room 402, Indianapolis, IN 46202, Tel: (317) 274-1036; xu26@iupui.edu. [*]Co-corresponding author: Riyi Shi, M.D., Ph.D., Professor, Department of Basic Medical Sciences, College of Veterinary Medicine, Weldon School of Biomedical Engineering, Purdue University, West Lafayette, IN 47907-1244, Tel: 765-496-3018 Fax: 765-494-7605; riyi@purdue.edu.
[#]These authors contributed equally to this work.

Disclosure Statement:
No competing financial interests exist.

infiltration. These results, combined with our previous reports, strongly suggest that acrolein may play a critical causal role in the pathogenesis of SCI and that targeting acrolein could be an attractive strategy for repair after SCI.

Keywords

Acrolein; Aldehyde; Oxidative stress; Lipid peroxidation; Spinal cord injury

INTRODUCTION

Traumatic spinal cord injury (SCI) leads to motor and sensory dysfunction below the level of injury. In the United States alone there were approximately 270,000 people living with SCI in 2012, and an additional 12,000 new cases occur every year, most of them younger than age 30 years (https://www.nscisc.uab.edu) (2012). Acute SCI initiates a complex cascade of molecular events termed 'secondary injury', which leads to progressive degeneration ranging from early neuronal apoptosis at the lesion site to delayed degeneration of intact white matter tracts, and, ultimately, expansion of the initial injury (Liu et al., 1997, Liu and Xu, 2012). Although the etiology and pathogenesis of SCI remain to be fully understood, evidence has shown that reactive oxygen species (ROS) and lipid peroxidation have a significant role in the pathophysiology of SCI (Hall and Braughler, 1986, Hall and Springer, 2004, Vaishnav et al., 2010, Liu and Xu, 2012). Lipid peroxidation involves free radical-induced oxidation of polyunsaturated fatty acids in cells and membrane phospholipids at allylic carbons (Vaishnav et al., 2010). As a consequence of lipid peroxidation-induced membrane damage, peroxidized fatty acids eventually lead to aldehydic breakdown products, including acrolein.

Acrolein, an α, β-unsaturated aldehyde, is highly reactive with many biomolecules including proteins, DNA, and phospholipids (Shi et al., 2011a). As both a product of and catalyst for lipid peroxidation, the highly reactive α, β-unsaturated aldehyde, acrolein, induces a vicious cycle of oxidative stress, dramatically amplifying its effects and perpetuating cellular damage (Shi et al., 2011a). Furthermore, it exhibits prolonged toxicity compared to other oxygen radicals within the body (Esterbauer et al., 1991, Ghilarducci and Tjeerdema, 1995, Luo et al., 2005) lasting for days rather than seconds (Ghilarducci and Tjeerdema, 1995, Evans and Halliwell, 1999). Previously, we demonstrated that acrolein was significantly increased in guinea pig spinal cord following a controlled compression SCI (Luo et al., 2005) and in rat spinal cord after contusive SCI (Park et al., 2014). To determine whether increased acrolein is sufficient to create damage in normal CNS tissue, a micro-amount of acrolein was injected into the rat thoracic spinal cord, which created cord tissue damage (Park et al., 2014). It remains unclear whether increased acrolein within the spinal cord could produce dose-dependent damage of tissue and loss of function. Here, we reported that acrolein induced significant dose-dependent damage to the spinal cord which correlated to a graded loss of behavioral function.

EXPERIMENTAL PROCEDURES

Animal care and microinjection

Adult female Sprague-Dawley rats weighing 200–250 g from Harlan Laboratory (Indianapolis, IN) were used in this study. All animals were maintained on a 12:12 light:dark schedule with food and water freely available. All animal surgical procedures and postoperative care protocols were performed in accordance with the Guide for the Care and Use of Laboratory Animals (National Research Council) and the Guidelines of the Indiana University School of Medicine Institutional Animal Care and Use Committee.

Animals received injections of saline, or acrolein (at two doses: 0.1 μmol or 1.0 μmol, Sigma, St. Louis, MO) and were kept for 24 h or 8 wk after the injection. Briefly, animals were anaesthetized using an intraperitoneal (IP) injection of ketamine (40 mg/kg)/xylazine (5 mg/kg). During the microinjection procedure, the dorsal surface of the spinal cord was exposed at the 10^{th} thoracic level (T10) and was injected at 0.6 mm from the midline and a depth of 1.3 mm from the dorsal cord surface using a stereotaxic device with a glass micropipette attached to a pneumatic picopump (World Precision Instruments, Inc., Sarasota, FL) (Fig. 1). In all cases, 1.0 μL of solution was injected over a period of at least 5 min. After injection, the needle was left in place for at least 2 min to allow for diffusion into the surrounding tissue. Muscle incisions were closed with silk sutures, and wound clips were used to close the skin. After surgery, all rats were returned to cages with clean bedding and placed on a heat pad. Each rat was given its own cage until it regained full consciousness. Once conscious, all rats were housed with rats of the same injury group. Bladders were manually voided until full recovery of function as needed.

Behavioral Assessments

All behavioral tests were blindly performed (n=8 rats/each group) according to our previous publications (Liu et al., 2006, Liu et al., 2007). **Basso, Beattie, and Bresnahan (BBB) locomotor rating scale:** The BBB scale was used to assess locomotor function of animals following injection procedures (Basso et al., 1995). Each rat was allowed to roam freely in an open field and was observed for 4 min by two scorers lacking knowledge of the experimental groups. The BBB scale was initially performed at 24 h after the microinjection to assess acute effects of the injury. Subsequently, testing was conducted once a week over a seven-week period to detect possible chronic effects. The BBB scale ranges from 0 (no discernible hind limb movement) to 21 (normal movement, including coordinated gait with parallel paw placement of the hind limb and consistent trunk stability). Scores from 0 to 7 show the recovery of isolated movements in the three joints (hip, knee, and ankle). Scores from 8 to 13 indicate the intermediate recovery phase showing stepping, paw placement, and forelimb-hind-limb coordination. Scores from 14 to 21 show the late phase of recovery with toe clearance during every step phase. BBB Scores of both assessors were averaged for each hind limb. For the unilateral acrolein injection, BBB scores of the ipsilateral hind limb were shown. No significant difference in BBB scores of the contralateral hind limb was found. **Grid walking:** The grid walking test was also used to assess hind limb locomotor deficits (Behrmann et al., 1992). During the test, rats were allowed to walk on a plastic mesh (3 × 3 sq ft) containing 4.5 × 5 cm diamond holes. Total hind limb footfalls were counted by two

observers unaware of the experimental groups during each trial. For testing, each animal was placed on the grid and allowed to perform the active grid walking task for a period of 3 min. During this time period, the number of footfalls (fall of the hind limb, including at least the ankle joint, through the grid surface) was determined individually for each hind limb.

Histology and immunohistochemistry

At 24 h and 8 wk after injection, animals were perfused for histological analysis. They received anesthesia with ketamine (80 mg/kg)/xylazine (10 mg/kg) and transcardial perfusion of 0.01 M Phosphate-buffered saline (PBS) followed by 4% paraformaldehyde (400 mL/rat). After perfusion, a 2-cm-long piece of the spinal cord was dissected out from each rat and left in the same fixative for 4 h, then transferred to 30% sucrose in 0.01M PBS (pH7.4). Spinal cord segments containing the epicenter were isolated from each animal, embedded, and cut into 20 μm-thick serial transverse sections in five identical sets. Two sets of the sections were stained for myelin with Luxol fast blue and counterstained with Cresyl violet-Eosin according to our previously described protocols (Liu et al., 2006, Liu et al., 2007). Cresyl violet-eosin stained slides were used to generate 3-dimensional reconstructions of spinal cord samples using an Olympus BX60 microscope equipped with a Neurolucida system (MicroBrightField, Colchester, VT). Spinal cord area, lesion area, grey matter area, and spared white matter (WM) area of the injured cord were manually traced by an observer and fed into a Neurolucida algorithm to estimate volumes of the given contours at 2,400 μm from the injury epicenter in both the rostral and the caudal directions. This resulted in 4,800 μm of total tissue scrutinized for 3-dimensional analysis. Luxol fast blue stained tissue was analyzed over the same distance using the same system. However, Luxol fast blue analysis included tracing only the cord area and the spared myelin area. The same Cresyl violet-eosin horizontal cross sections used for assessing lesion volume were used to count the number of ventral motoneurons in the spinal cord epicenter region at 24 h and 8 wk (Walker et al., 2012). A horizontal line was drawn across the transverse section of spinal cord tissue at the level of the central canal. All ipsilateral motoneurons ventral to the horizontal line were manually quantified using ImageJ software. Only clearly identifiable motoneurons with appropriately dark and even cresyl violet stained nuclei were counted.

The other sets of sections from rats perfused at 24 h and 8 wk post-injection were immunostained with ectodermal dypslasia (ED1, a macrophage marker) and anti-glial fibrillary acidic protein (GFAP, an astrocyte marker) according to a previously described protocol (Liu et al., 2006, Liu et al., 2011). The primary antibodies used included the polyclonal rabbit anti-GFAP (1:200, Sigma), and monoclonal mouse anti-ED1 (1:100, AbD Serotec, Raleigh, NC). The secondary antibodies used included fluorescein-conjugated goat anti-rabbit (1:100; ICN Biochemicals, Aurora, OH) and rhodamine-conjugated goat anti-mouse (1:100; ICN Biochemicals) antibodies. Hoechst 33342 (1:100) was added as a nuclear stain during subsequent PBS washes.

Electron microscopy

Tissue preparation for electron microscopy was described in our previous publication (Liu et al., 2006, Liu et al., 2011). Briefly, spinal cord segments were fixed overnight in the solution containing 2% glutaraldehyde and 5% sucrose in 0.1 M sodium cacodylate buffer, pH 7.4,

followed by 1% osmium tetroxide in the same buffer for 1 h. The tissue was embedded in Spurr's epoxy resin and cured at 70°C. Observation areas were determined by transverse semi-thin sections (1 μm) which were first stained with a mixture of 1% toluidine blue and 1% sodium borate. Ultra-thin sections (70–90 nm) were collected on copper mesh grids with 600 bars per inch, subsequently counterstained with 4 % uranyl acetate in 50 % ethanol, and Reynolds' lead citrate, and examined using a Philip 400 transmission electron microscope.

Statistical Analysis

All statistical analyses were performed using GraphPad Prism software (version 6.00, La Jolla California USA). All data were presented as mean ± s.e.m values, and were analyzed by analyses of variance (ANOVA) (one-way, two-way, or repeated-measures as appropriate) followed by *post hoc* Dunnett's or Tukey's multiple comparison test. A p value of <0.05 was considered statistically significant.

RESULTS

Acrolein induced spinal cord functional impairment in a dose-dependent manner

To determine whether micro-amounts of acrolein would induce dose-dependent functional impairments, we microinjected acrolein (two doses at 0.1 and 1.0 μmol) into the normal spinal cord of adult rats and performed both BBB locomotor rating scale and grid walking analyses. The BBB scale is a sensitive and reliable method for detecting differences in locomotion across multiple injury severities after SCI (Basso et al., 1995, 1996). BBB scores were reduced after the injection of acrolein (Fig. 2). Clearly, as the doses of acrolein used increased, the BBB scores obtained decreased. At 24 h, rats that received both 0.1 and 1.0 μmol of acrolein exhibited significantly lower BBB scores than rats that received saline injection. One week later, rats injected with 0.1 μmol of acrolein no longer displayed significantly lower BBB scores compared to saline-injected rats. The rats injected with 1.0 μmole acrolein, however, continued to display significantly lower BBB scores for the entire 7 week testing period. Furthermore, rats injected with 1.0 μmol acrolein had significantly lowered BBB scores than rats injected with 0.1 μmole of acrolein at all the time points studied.

Hind limb locomotor function was also assessed using grid walk testing. None of the injury groups displayed any significant increase in hind limb foot drops on their uninjected side during the testing period (Fig. 3B). However, on the injected side, acrolein injection induced dose-dependent foot drops (Fig. 3A). The significant difference in foot drops between the low dose and vehicle-treated groups was found only at 24 h post-injection. However, significant differences in foot drops were found between the high dose and low dose acrolein-treated groups and between the high dose and saline-treated groups in most time points (Fig. 3A).

Acrolein induced spinal cord tissue damage in a dose-dependent manner

Because we showed that microinjections of acrolein induced dose-dependent functional impairments, we next examined whether such microinjected acrolein also would result in dose-dependent tissue damage. Histological staining was visually scrutinized for abnormal

properties in the microinjected tissue. At 24 h, cresyl violet staining revealed moderate and severe damage to both the white and grey matter, as well as motoneuron loss and cord swelling (Fig. 4). Stereological analyses further demonstrated that volumetric tissue damage was significantly increased in a dose- dependent manner after microinjections of acrolein (Fig. 4G–J). Luxol fast blue staining showed that acrolein injection induced white matter demyelination in a dose-dependent manner at 24 h (Fig. 4A–C, K). Ipsilateral to contralateral cord ratio was determined to give a numerical approximation of swelling or shrinkage of microinjected cords. A significant increase in ipsilateral to contralateral cord ratio occurred in animals injected with 0.1 and 1.0 μmol acrolein when compared to saline at 24 h in Cresyl Violet stained tissue (Fig. 4L), suggesting spinal cord swelling after acrolein injection. Motoneurons, important for motor function, were counted to gauge the level of acrolein injection-induced damage. A bar graph demonstrates that motor neuron loss was significantly increased in a dose-dependent manner at 24 h after the injection (Fig. 4M). As expected, no apparent tissue damage was found in rats that received saline injection (Fig. 4A and D).

At the 8th wk, cresyl violet staining revealed moderate and severe damage to both white and grey matter, loss of motoneurons and cord shrinkage after the 0.1 and 1.0 μmol acrolein injections (Fig. 5). A dose-dependent lesion volume (Fig. 5G–J) and white matter demyelination (Fig. 5A–C, K) were also detected at 8 wk after the two doses of acrolein injections. In contrast to 24 h after the injections, cord shrinkage was observed at 8 wk after the acrolein injections (Fig. 5L). A bar graph also shows that motoneuron loss was significantly increased in a dose-dependent manner at 8 wk after the acrolein injection (Fig. 5M). Immunofluorescence staining revealed an increase in GFAP expression (Fig. 6A–F) near the lesion border and an increase in ED-1 expression (Fig. 6G–L) within the lesion site at 8 wk after acrolein injection, suggesting that acrolein induced reactive gliosis and inflammation.

Electron microscopy showed relatively healthy, myelin wrapped axons in saline injected animals at 24 h (Fig. 7A) and 8 wk (Fig. 7D). Injection of 0.1 μmol acrolein resulted in thinning of myelin (Fig. 7B) or degeneration (Fig. 7E) of axons at 24 h and 8 wk post-injection. Injection of 1.0 μmol acrolein showed axon degeneration, large axons with thin myelin, and microphage infiltration at 24 h (Fig. 7C) and 8 wk (Fig. 7F) post-injection. The presence of large axons with thin myelin or without myelin suggests demyelination or myelin dysfunction.

DISCUSSION

In the present study, we show that injection of micromole acrolein into the normal spinal cord is sufficient to induce dose-dependent spinal cord tissue damage. This tissue pathology correlates well with a dose-dependent loss of behavioral function. Immunofluorescence staining revealed that acrolein injection directly induced gliotic response and inflammation. Ultrastructurally, acrolein injection induced axonal degeneration, demyelination, and macrophage invasion. Previously, it was reported that, following SCI, acrolein was significantly increased and peaked at 24 h post-injury (Luo et al., 2005, Park et al., 2014). Hydralazine, a known acrolein scavenger, alleviated acrolein-mediated neuronal damage *in*

vitro (Liu-Snyder et al., 2006a, Hamann et al., 2008a, Hamann et al., 2008b), and reduced tissue damage, and motor deficits after SCI *in vivo* (Park et al., 2014). Collectively, these results strongly indicate that acrolein may play a critical causal role in the pathogenesis of spinal cord secondary damage.

Acrolein, a byproduct of lipid peroxidation, is the strongest electrophile among the unsaturated aldehydes (Esterbauer et al., 1991, Shi et al., 2011a) and occurs at 40 times greater concentration than other α, β-unsaturated aldehydes such as 4-hydroxynonenal (4-HNE) (Esterbauer et al., 1991). Although increased acrolein was observed in the injury cord after SCI (Luo et al., 2005), the exact concentration of acrolein within the injured spinal cord has not been quantified. Increasing evidence suggests that μM-mM levels of acrolein are likely to occur in the pathological tissue (Nardini et al., 2002, Sakata et al., 2003, Shi et al., 2011a). For example, it has been estimated that acrolein accumulation in the hippocampus of human Alzheimer's patients could reach 500 μM (Lovell et al., 2001, Hamann et al., 2008b). It has also been reported that acrolein-lysine adducts could reach up to 1.24 mM in human urine (Satoh et al., 1999). Although the knowledge of exact diffusion patterns for specific compounds within CNS tissue is limited, establishing a relationship between tissue volume and injection diffusion has been attempted. It has been estimated that a volume of 1 μL solution will diffuse up to a distance of 2.2 mm in any given direction measured as early as 10 minutes after injection in brain (Myers, 1966). Based on our measurements, the diameter of spinal cord of living rat is measured to be about 4 mm. Therefore, the transverse area of spinal cord is about 12.5 mm^2 (assuming the transverse area is circular). Consequently, the volume of spinal cord covering such distance (2.2 mm) is about $12.5 \times 2.2 = 27.5$ mm^3 which is equivalent to 27.5 μL. In the case of using a dosage of 0.1 μmol (in 1 μL), the average possible final concentration of acrolein in such area shortly after injection could be about 3.36 mM, with a volume dilution of 27.5 times from the original injecting volume of 1 μL.

Due to the known limitation of currently available measuring techniques, the reported literature measures of acrolein concentrations in vivo are likely underestimations. For example, in one of the most common techniques for measuring acrolein, the detection of acrolein-lysine adducts, the antibody was developed to only recognize proteins bearing acrolein-bound lysine residues (Uchida et al., 1998). However, it is well known that acrolein is equally capable of attacking cysteine, histidine, and arginine moieties (Esterbauer et al., 1991, Stevens and Maier, 2008). Actually, it has been estimated that acrolein's affinity for cysteine is higher than lysine (LoPachin et al., 2008). Consequently, acrolein-lysine adducts may only account for a fraction of the total acrolein-protein adducts. Therefore, it is reasonable to speculate that the acrolein detection using antibodies that only recognize acrolein-lysine adducts (but not acrolein-cysteine, acrolein-arginine, or acrolein-histidine adducts) is an underestimation of total acrolein-protein adducts. Taken together, it is obvious that the concentration we used in this initial investigation is on the high end of the range measured in vivo. However, considering the fact that the actual acrolein concentration may be significantly higher than what has been measured (due to the limitation of the current methods), it is possible that the concentration we used during this exploratory study may be closer to reality than it appears. In addition, it is worth mentioning that the toxicity of acrolein is time-dependent, and acrolein is likely to be present for long periods of time (on

the order of weeks post-injury) in physiologically compromised tissue, such as that found in the mechanically injured spinal cord (Park et al., 2014). However, in the current study examining its immediate damage in healthy tissue, the spinal cord was exposed to acrolein for a much shorter time. Therefore, the present experimental design may justify the usage of high dosage of acrolein aiming to recapitulate acrolein-mediated damage in vivo. In future studies, it may be a useful endeavor to gradually infuse lower acrolein loads over an extended time period.

One fact that further supports the relevance of the dosage of acrolein used in this investigation is that, acrolein microinjection with selected low and high dose induced injury pathology and functional deficits similar to what we observed after a classical spinal cord injury (Liu et al., 2006, Liu et al., 2007, Park et al., 2014). To our knowledge, this is the first time that dose-dependent tissue damage and functional impairment was observed after single injections of acrolein into the normal adult rat spinal cord. This suggests that acrolein alone is sufficient to induce spinal cord damage, a process similar to what we observed after a mechanical trauma to the spinal cord within which high levels of acrolein are found.

The acrolein injection caused significant diffusive injury in the spinal cord as shown in Figures 4 (G–I) and 5 (G–I). The rostral and caudal diffusion of tissue injury instigated by acrolein was demonstrated first in Figure 4 (24 hours post injection), and to a greater extent, in Figure 5 (8 weeks post injection). A further point worth mentioning here is that the diffusive and regenerative injury caused by acrolein in the current study is, if different than in SCI, an underestimation compared to in vivo SCI. This is because acrolein injury can be synergistically exacerbated or fueled by other parallel injuries seen in SCI (Peasley and Shi, 2003). In the current proof-of-principle experiment, acrolein was the only pathological initiating factor and no physical impact was imparted onto the spinal cord. Therefore, it is reasonable to speculate that acrolein-mediated injury seen in the current study would be significantly more severe, diffusive, regenerative, and long lasting if combined with concomitant physical trauma and other secondary injury factors.

A noteworthy finding of this study is that acrolein injection induced spinal cord motor neuron loss in which acrolein was used as the only source of a damage factor. Given that SCI induces a rapid increase and prolonged concentration of acrolein (Luo et al., 2005) and that acrolein is highly reactive with proteins, DNA, and phospholipids (Shi et al., 2011a), it is conceivable that increased levels of acrolein may directly induce neuronal death. This is supported by the observation that the acrolein induced death of cultured PC12 cells, dorsal root ganglion cells and hippocampal neurons (Lovell et al., 2001, Liu-Snyder et al., 2006a, Liu-Snyder et al., 2006b). In addition to its direct effect on neuronal death, acrolein may trigger a cascade of downstream events, which lead to indirect neuronal death. Indeed, both previous and current studies demonstrated that acrolein could induce inflammation and PLA_2 activation (Fukuda et al., 1999, Park and Taniguchi, 2008) which, in turn, induce neuronal death indirectly (Liu et al., 2006, Liu et al., 2007, Liu and Xu, 2012). Thus, acrolein likely serves as a key molecule that mediates neuronal death in both direct and indirect manners.

In this study, more ventral motoneurons were found at multiple distances from the injury epicenter in the 8 wk post-injury group than the 24 h post-injury group in cresyl violet-stained sections. The presence of more ventral motoneurons at the 8 wk time point does not necessarily mean that these neurons were regenerated. Rather, they might represent a population of neurons that transiently lost Nissl substances in response to an acute injury (24 h). The Nissl substance, composed of fragments of endoplasmic reticulum with adhering ribosomes that are the staining target for cresyl violet, may have been denatured at 24 h, which made those motoneurons invisible at this time point. At 8 wk post-injury (Figure 5), those motoneurons which have not undergone degeneration and truly have disappeared may have recovered sufficiently to become visible again in regards to cresyl violet staining, as well as regaining their function as judged by recovery of their BBB scores and fewer foot drops.

Another noteworthy observation in this study was that acrolein injection induced a rapid and confined demyelination. This is evidenced by the lack of myelin staining in the ventrolateral white matter surrounding the injection site, the reduction of myelinated axons in the same region, and the presence of a large quantity of axons with thin myelin at the EM level. These results, along with the observation that acrolein can cause significant myelin damage in isolated guinea pig spinal cord (Shi et al., 2011b), collectively imply that acrolein is a molecule that could induce CNS demyelination. Based on the degradation of myelin basic protein observed in our previous study at the paranodal region (Shi et al., 2011b), it is likely that acrolein reacts directly with myelin basic protein, which leads to myelin damage (Readhead et al., 1990, Boggs, 2006). It remains unclear, however, whether this demyelination results from a direct attack of acrolein on the CNS myelin or an indirect effect caused by acrolein-mediated PLA_2 activation and macrophage invasion. Myelin damage can lead to the loss of axonal conduction and paralysis in SCI (Blight, 1985, 1991, Totoiu and Keirstead, 2005).

Reactive gliosis and inflammation have been considered as two major characteristics of SCI. Our observation that acrolein-induced astrocyte reaction and macrophage invasion in the spinal cord further indicates that acrolein is involved in the secondary injury after SCI.

In conclusion, our study demonstrates that acrolein induced dose-dependent spinal cord tissue damage with astrocytic gliotic response and macrophage invasion. Such tissue damage was accompanied by corresponding functional impairment in a dose-dependent manner. These findings suggest that acrolein may play a critical causal role in the pathogenesis of spinal cord injury. Furthermore, the molecular mechanisms underlying the action of acrolein and its regulation after SCI need to be elucidated. Experiments along these lines are currently in progress in our laboratory.

Acknowledgments

We thank Tom Verhovshek for technical assistance and Ms. Patti Raley, a medical editor, for her critical reading of the manuscript. This work was supported by NIH NS073636 (RS/XMX), NS059622, DOD CDMRP W81XWH-12-1-0562, DVA 1I01BX002356-01A1, Craig H Neilsen Foundation 296749, Indiana Spinal Cord and Brain Injury Research Foundation and Mari Hulman George Endowment Funds (XMX), and by the State of Indiana (ISDH, Grant # A70-2-079609, A70-9-079138 and A70-5-0791033; NKL). We are grateful for the use of the Core

facility of the Spinal Cord and Brain Injury Research Group/Stark Neurosciences Research Institute at Indiana University.

Abbreviations

SCI	spinal cord injury
BBB	Basso, Beattie, and Bresnahan locomotor rating scale
IP	intraperitoneal
GFAP	anti-glial fibrillary acidic protein
ED1	ectodermal dysplasia
ANOVA	analysis of variance
PBS	Phosphate-buffered saline

References

1. Spinal cord injury facts and figures at a glance. J Spinal Cord Med. 2012; 35:480–481. [PubMed: 23318031]
2. Basso DM, Beattie MS, Bresnahan JC. A sensitive and reliable locomotor rating scale for open field testing in rats. J Neurotrauma. 1995; 12:1–21. [PubMed: 7783230]
3. Basso DM, Beattie MS, Bresnahan JC. Graded histological and locomotor outcomes after spinal cord contusion using the NYU weight-drop device versus transection. Exp Neurol. 1996; 139:244–256. [PubMed: 8654527]
4. Behrmann DL, Bresnahan JC, Beattie MS, Shah BR. Spinal cord injury produced by consistent mechanical displacement of the cord in rats: behavioral and histologic analysis. J Neurotrauma. 1992; 9:197–217. [PubMed: 1474608]
5. Blight AR. Delayed demyelination and macrophage invasion: a candidate for secondary cell damage in spinal cord injury. Cent Nerv Syst Trauma. 1985; 2:299–315. [PubMed: 3836014]
6. Blight AR. Morphometric analysis of a model of spinal cord injury in guinea pigs, with behavioral evidence of delayed secondary pathology. J Neurol Sci. 1991; 103:156–171. [PubMed: 1880533]
7. Boggs JM. Myelin basic protein: a multifunctional protein. Cell Mol Life Sci. 2006; 63:1945–1961. [PubMed: 16794783]
8. Esterbauer H, Schaur RJ, Zollner H. Chemistry and biochemistry of 4-hydroxynonenal, malonaldehyde and related aldehydes. Free Radic Biol Med. 1991; 11:81–128. [PubMed: 1937131]
9. Evans P, Halliwell B. Free radicals and hearing. Cause, consequence, and criteria. Ann N Y Acad Sci. 1999; 884:19–40. [PubMed: 10842581]
10. Fukuda T, Kim DK, Chin MR, Hales CA, Bonventre JV. Increased group IV cytosolic phospholipase A2 activity in lungs of sheep after smoke inhalation injury. Am J Physiol. 1999; 277:L533–542. [PubMed: 10484460]
11. Ghilarducci DP, Tjeerdema RS. Fate and effects of acrolein. Rev Environ Contam Toxicol. 1995; 144:95–146. [PubMed: 8599034]
12. Hall ED, Braughler JM. Role of lipid peroxidation in post-traumatic spinal cord degeneration: a review. Cent Nerv Syst Trauma. 1986; 3:281–294. [PubMed: 3555850]
13. Hall ED, Springer JE. Neuroprotection and acute spinal cord injury: a reappraisal. NeuroRx. 2004; 1:80–100. [PubMed: 15717009]
14. Hamann K, Durkes A, Ouyang H, Uchida K, Pond A, Shi R. Critical role of acrolein in secondary injury following ex vivo spinal cord trauma. J Neurochem. 2008a; 107:712–721. [PubMed: 18710419]

15. Hamann K, Nehrt G, Ouyang H, Duerstock B, Shi R. Hydralazine inhibits compression and acrolein-mediated injuries in ex vivo spinal cord. J Neurochem. 2008b; 104:708–718. [PubMed: 17995940]
16. Liu-Snyder P, Borgens RB, Shi R. Hydralazine rescues PC12 cells from acrolein-mediated death. J Neurosci Res. 2006a; 84:219–227. [PubMed: 16619236]
17. Liu-Snyder P, McNally H, Shi R, Borgens RB. Acrolein-mediated mechanisms of neuronal death. J Neurosci Res. 2006b; 84:209–218. [PubMed: 16619238]
18. Liu NK, Titsworth WL, Zhang YP, Xhafa AI, Shields CB, Xu XM. Characterizing phospholipase A2-induced spinal cord injury-a comparison with contusive spinal cord injury in adult rats. Transl Stroke Res. 2011; 2:608–618. [PubMed: 23585818]
19. Liu NK, Xu XM. Neuroprotection and its molecular mechanism following spinal cord injury. Neural regeneration research. 2012; 7:2051–2062. [PubMed: 25624837]
20. Liu NK, Zhang YP, Han S, Pei J, Xu LY, Lu PH, Shields CB, Xu XM. Annexin A1 reduces inflammatory reaction and tissue damage through inhibition of phospholipase A2 activation in adult rats following spinal cord injury. J Neuropathol Exp Neurol. 2007; 66:932–943. [PubMed: 17917587]
21. Liu NK, Zhang YP, Titsworth WL, Jiang X, Han S, Lu PH, Shields CB, Xu XM. A novel role of phospholipase A2 in mediating spinal cord secondary injury. Ann Neurol. 2006; 59:606–619. [PubMed: 16498630]
22. Liu XZ, Xu XM, Hu R, Du C, Zhang SX, McDonald JW, Dong HX, Wu YJ, Fan GS, Jacquin MF, Hsu CY, Choi DW. Neuronal and glial apoptosis after traumatic spinal cord injury. J Neurosci. 1997; 17:5395–5406. [PubMed: 9204923]
23. LoPachin RM, Barber DS, Gavin T. Molecular mechanisms of the conjugated alpha,beta-unsaturated carbonyl derivatives: relevance to neurotoxicity and neurodegenerative diseases. Toxicol Sci. 2008; 104:235–249. [PubMed: 18083715]
24. Lovell MA, Xie C, Markesbery WR. Acrolein is increased in Alzheimer's disease brain and is toxic to primary hippocampal cultures. Neurobiol Aging. 2001; 22:187–194. [PubMed: 11182468]
25. Luo J, Uchida K, Shi R. Accumulation of acrolein-protein adducts after traumatic spinal cord injury. Neurochem Res. 2005; 30:291–295. [PubMed: 16018572]
26. Myers RD. Injection of Solutions into Cerebral Tissue: Relation between Volume and Diffusioff. Physiol Behav. 1966; 1:171–174.
27. Nardini M, Finkelstein EI, Reddy S, Valacchi G, Traber M, Cross CE, van der Vliet A. Acrolein-induced cytotoxicity in cultured human bronchial epithelial cells. Modulation by alpha-tocopherol and ascorbic acid. Toxicology. 2002; 170:173–185. [PubMed: 11788155]
28. Park J, Zheng L, Marquis A, Walls M, Duerstock B, Pond A, Vega-Alvarez S, Wang H, Ouyang Z, Shi R. Neuroprotective role of hydralazine in rat spinal cord injury-attenuation of acrolein-mediated damage. J Neurochem. 2014; 129:339–349. [PubMed: 24286176]
29. Park YS, Taniguchi N. Acrolein induces inflammatory response underlying endothelial dysfunction: a risk factor for atherosclerosis. Ann N Y Acad Sci. 2008; 1126:185–189. [PubMed: 18448814]
30. Peasley MA, Shi R. Ischemic insult exacerbates acrolein-induced conduction loss and axonal membrane disruption in guinea pig spinal cord white matter. J Neurol Sci. 2003; 216:23–32. [PubMed: 14607299]
31. Readhead C, Takasashi N, Shine HD, Saavedra R, Sidman R, Hood L. Role of myelin basic protein in the formation of central nervous system myelin. Ann N Y Acad Sci. 1990; 605:280–285. [PubMed: 1702601]
32. Sakata K, Kashiwagi K, Sharmin S, Ueda S, Irie Y, Murotani N, Igarashi K. Increase in putrescine, amine oxidase, and acrolein in plasma of renal failure patients. Biochem Biophys Res Commun. 2003; 305:143–149. [PubMed: 12732208]
33. Satoh K, Yamada S, Koike Y, Igarashi Y, Toyokuni S, Kumano T, Takahata T, Hayakari M, Tsuchida S, Uchida K. A 1-hour enzyme-linked immunosorbent assay for quantitation of acrolein- and hydroxynonenal-modified proteins by epitope-bound casein matrix method. Anal Biochem. 1999; 270:323–328. [PubMed: 10334850]

34. Shi R, Rickett T, Sun W. Acrolein-mediated injury in nervous system trauma and diseases. Mol Nutr Food Res. 2011a; 55:1320–1331. [PubMed: 21823221]

35. Shi Y, Sun W, McBride JJ, Cheng JX, Shi R. Acrolein induces myelin damage in mammalian spinal cord. J Neurochem. 2011b; 117:554–564. [PubMed: 21352229]

36. Stevens JF, Maier CS. Acrolein: sources, metabolism, and biomolecular interactions relevant to human health and disease. Mol Nutr Food Res. 2008; 52:7–25. [PubMed: 18203133]

37. Totoiu MO, Keirstead HS. Spinal cord injury is accompanied by chronic progressive demyelination. The Journal of comparative neurology. 2005; 486:373–383. [PubMed: 15846782]

38. Uchida K, Kanematsu M, Sakai K, Matsuda T, Hattori N, Mizuno Y, Suzuki D, Miyata T, Noguchi N, Niki E, Osawa T. Protein-bound acrolein: potential markers for oxidative stress. Proc Natl Acad Sci U S A. 1998; 95:4882–4887. [PubMed: 9560197]

39. Vaishnav RA, Singh IN, Miller DM, Hall ED. Lipid peroxidation-derived reactive aldehydes directly and differentially impair spinal cord and brain mitochondrial function. J Neurotrauma. 2010; 27:1311–1320. [PubMed: 20392143]

40. Walker CL, Walker MJ, Liu NK, Risberg EC, Gao X, Chen J, Xu XM. Systemic bisperoxovanadium activates Akt/mTOR, reduces autophagy, and enhances recovery following cervical spinal cord injury. PLoS One. 2012; 7:e30012. [PubMed: 22253859]

Highlights

- Acrolein microinjection produces dose-dependent tissue damage and motor deficits.
- Acrolein microinjection induces gliotic response and macrophage invasion.
- Acrolein could be an important contributor to secondary spinal cord injury.
- Acrolein could be a target for therapeutic intervention.

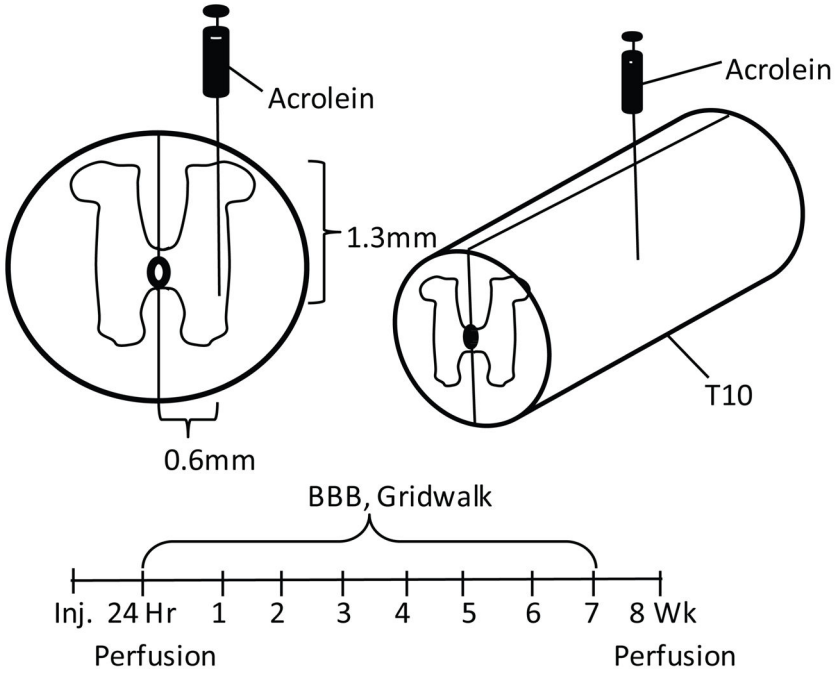

Figure 1.

Diagram of microinjection and experimental timeline. Saline or acrolein was injected into the rat spinal cord at a depth of 1.3 mm and a distance of 0.6 mm lateral from the midline at T10. Basso, Beattie, and Bresnahan (BBB) locomotor rating scale and grid walking tests were performed prior to the injection procedure, 24 h after injection, and then once a week for 7 wk. Animals were sacrificed at 24 h (acute observation) and 8 wk (chronic observation), respectively, after the injection.

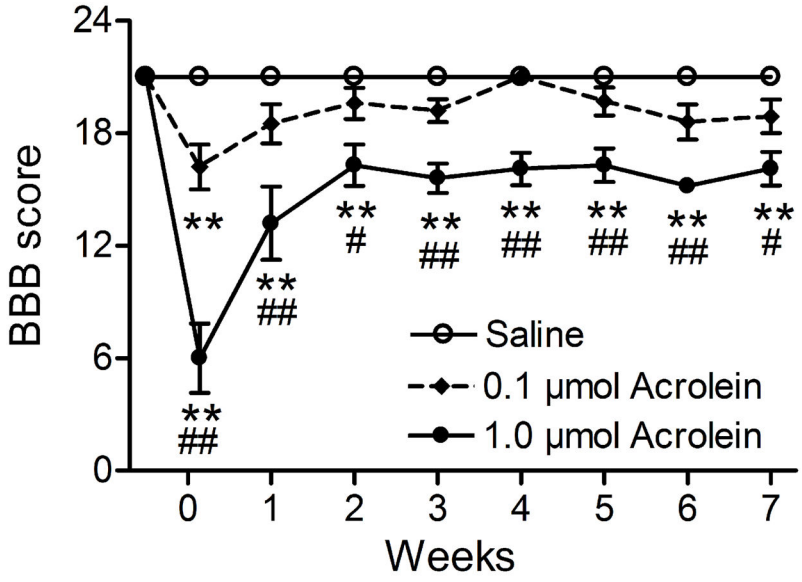

Figure 2.

Basso, Beattie, and Bresnahan (BBB) locomotor rating scale score over 7 wk after injections of acrolein into the normal spinal cord of adult rats. The BBB locomotion rating scale showed that BBB scores decreased in response to increased doses of acrolein (**: $p<0.01$, vs saline; #: $p<0.05$, ##: $p<0.01$, vs 0.1μmol acrolein).

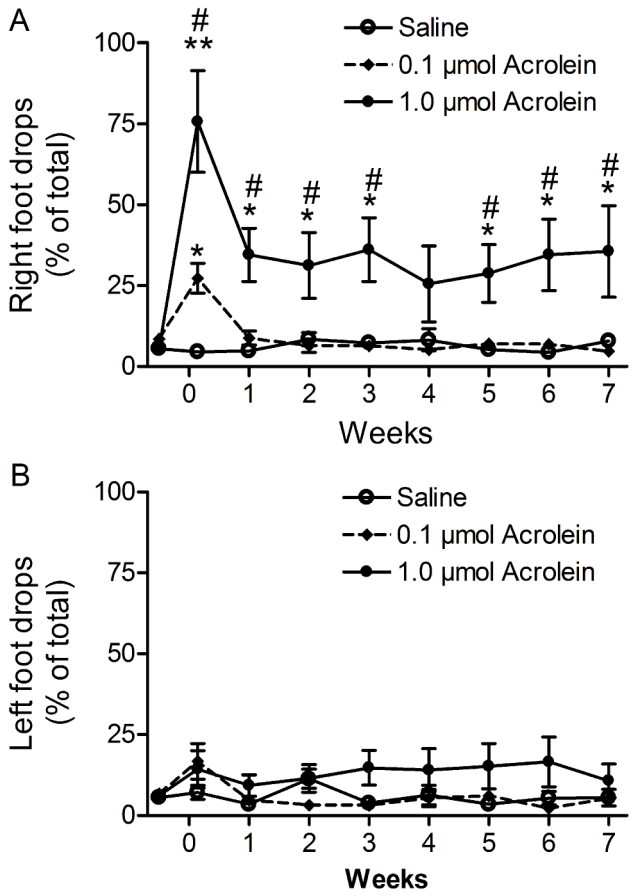

Figure 3.

Foot drops via grid walking test over 7 wk after injections of acrolein into the normal adult rat spinal cord on the right side at T10. (A) Significant increases of foot drops on the side ipsilateral to the acrolein injection were found in both doses (0.1 and 1.0 µmol) at 24 h after the injection. At most time points (except for the 4th wk), injection of high dose acrolein (1.0 µmol) resulted in significantly greater foot drops on the injury side than the low dose (0.1 µmol) or saline control (*: $p<0.05$,**: $p<0.01$, vs saline; #: $p<0.05$, vs 0.1µmol acrolein). (B) The foot drops on the side contralateral to the injection showed no difference amongst groups.

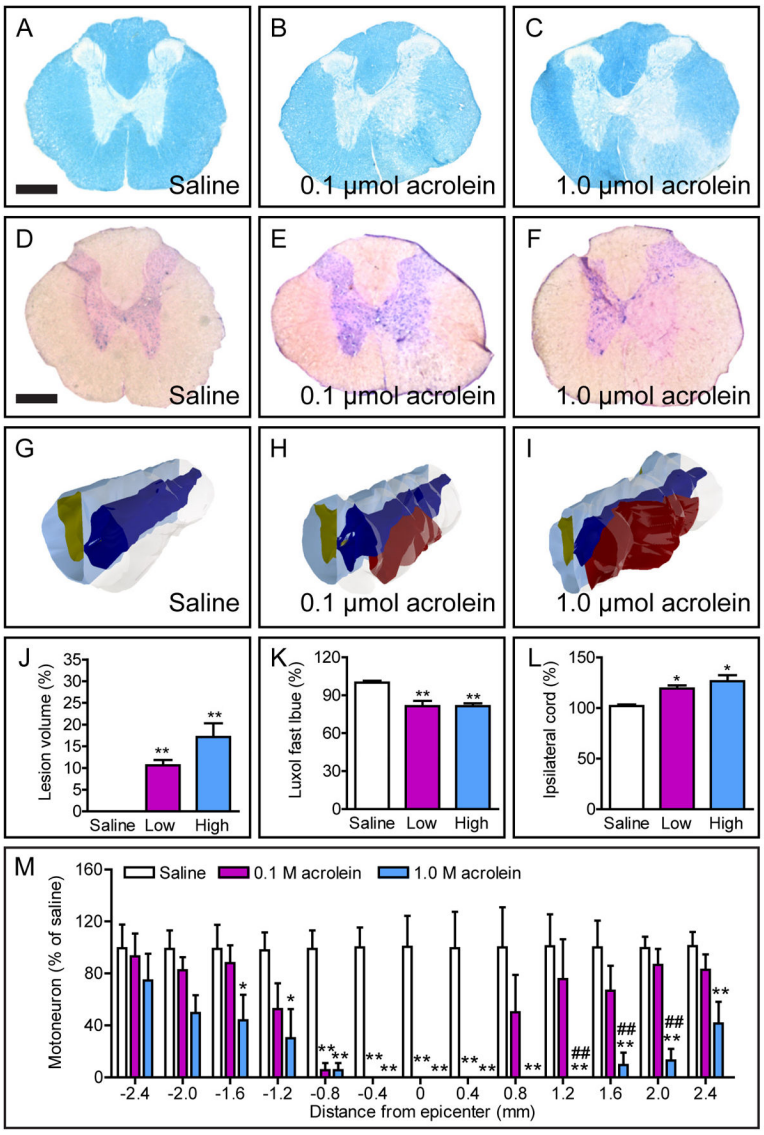

Figure 4.

Acrolein induced graded tissue damage at 24 h after injection. (**A, D**) Luxol fast blue (A) and Cresyl violet-eosin (D) stainings show no tissue damage or demyelination in a saline-injected spinal cord. (**B, C, E, F**) Low (0.1 µmol, B, E) and high dose (1.0 µmol, C, F) acrolein injections induced a confined lesion and demyelination in the ventral and ventrolateral grey and white matter. Bars: A–F, 500 µm. (**G–I**) Representative three-dimensional reconstruction of a spinal cord segment from each group illustrates rostrocaudal extension of the lesion (red). (**J–L**) Bar graphs show acrolein injection induced percent changes in lesion volume (J), demyelination (K), and cord swelling (L) among the three groups (Low, 0.1 µmol acrolein; High, 1.0 µmol acrolein; *: $p<0.05$,**: $p<0.01$, vs saline). (M) Acrolein injections into the right spinal cord cause significant dose-related motoneuron loss (*: $p<0.05$, **: $p<0.01$, vs saline; ##: $p<0.01$, vs 0.1µmol acrolein).

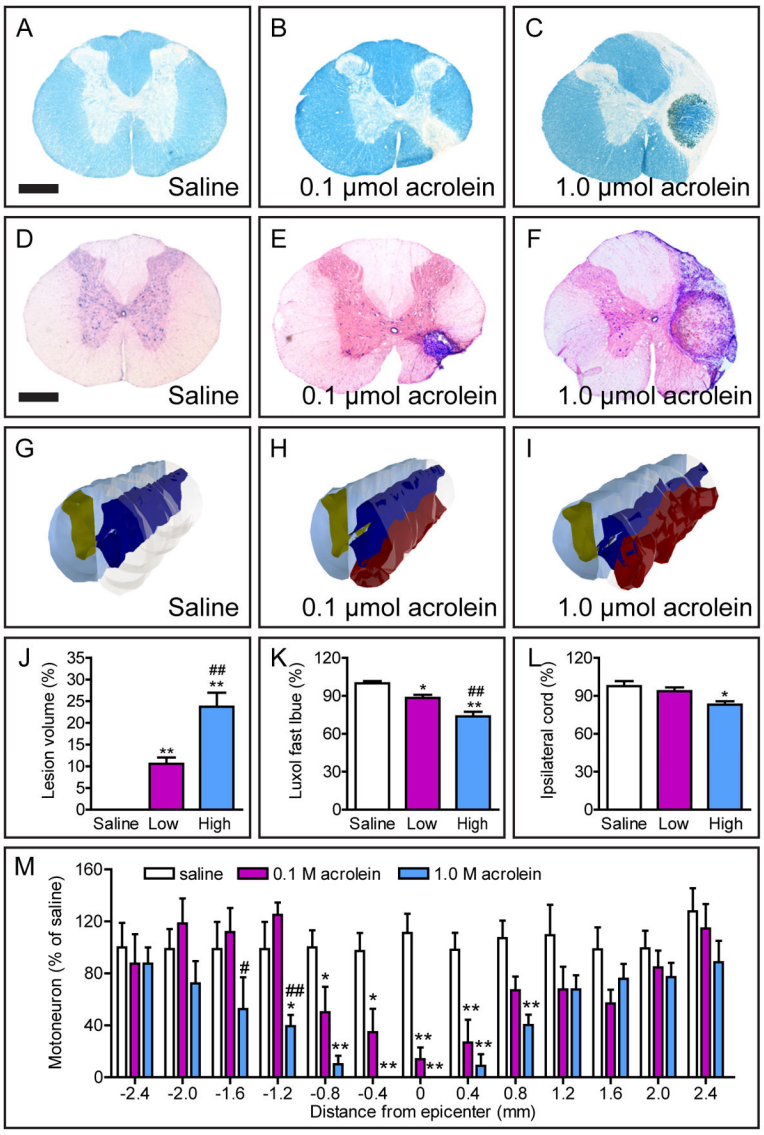

Figure 5.

Injections of acrolein into the normal spinal cord resulted in tissue damage in a dose-dependent manner at 8 wk. (**A, D**) Luxol fast blue (A) and Cresyl violet-eosin (D) stainings showed no tissue damage or demyelination in a saline-injected spinal cord. (**B, C, E, F**) Low (0.1 µmol, B, E) and high dose (1.0 µmol, C, F) acrolein injections induced a confined lesion and demyelination in the ventral and ventrolateral grey and white matter. Bars: A–F, 500 µm. (**G–I**) Representative three-dimensional reconstruction of a spinal cord segment from each group illustrates rostrocaudal extension of the lesion (red). (**J–L**) Bar graphs show acrolein injection induced percent changes in lesion volume (J), demyelination (K), and cord swelling (L) among the three groups (Low, 0.1 µmol acrolein; High, 1.0 µmol acrolein; *: $p<0.05$,**: $p<0.01$, vs saline; ##: $p<0.01$, vs 0.1 µmole acrolein). (**M**) Acrolein injections into the right spinal cord caused significant dose-related motoneuron loss (*: $p<0.05$, **: $p<0.01$, vs saline; #: $p<0.05$, ##: $p<0.01$, vs 0.1 µmole acrolein).

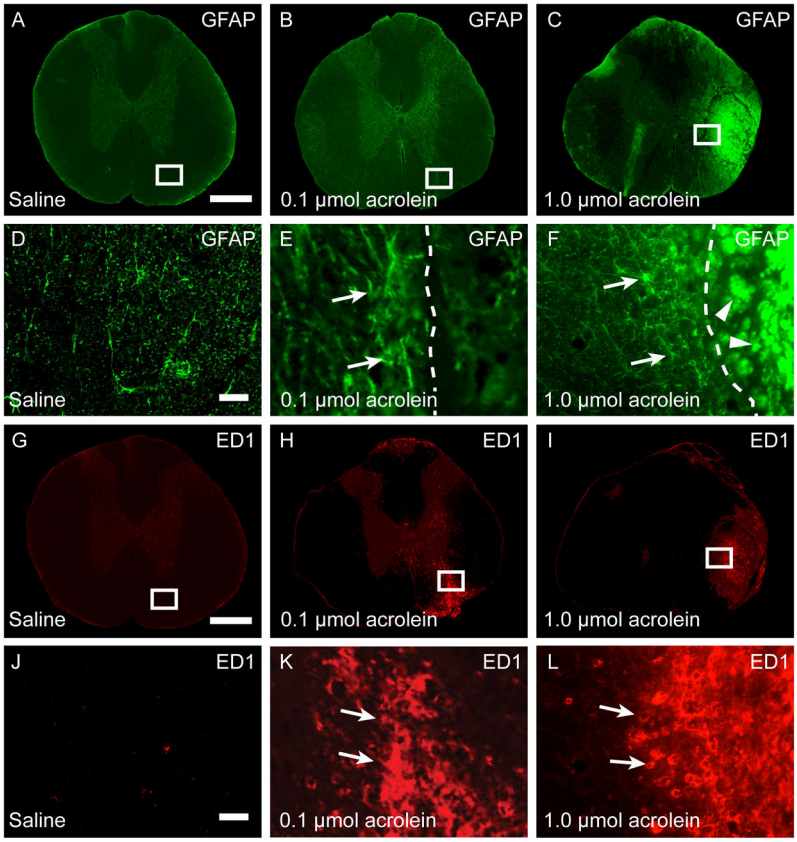

Figure 6.

Immunofluorescence staining at 8th wk after acrolein injection. (**A–F**) Increased GFAP expression at the lesion border shows acrolein-induced reactive gliosis in both low (0.1 μmol) and high (1.0 μmol) doses of acrolein injection groups. (**D–F**) High magnification of boxed areas in A-C shows normal (D) and reactive (E, F, arrows) astrocytes. Within the lesion epicenter, non-specifically labeled, morphologically characteristic of macrophages were also found (F, arrowheads). (G–I) Representative photomicrographs show increased ED-1 expression, a macrophage marker, within the lesion site of low and high doses of acrolein injections. (**J–L**) High magnification of boxed areas of G–I showed the lack of (J) or presence of (K, L, arrows) macrophages stained with ED-1 after saline (J) or acrolein (K, L) injections. The invaded macrophages were confined mainly within the lesion site. Bars: A–C and G–I, 500 μm; D–F and J–L, 40 μm.

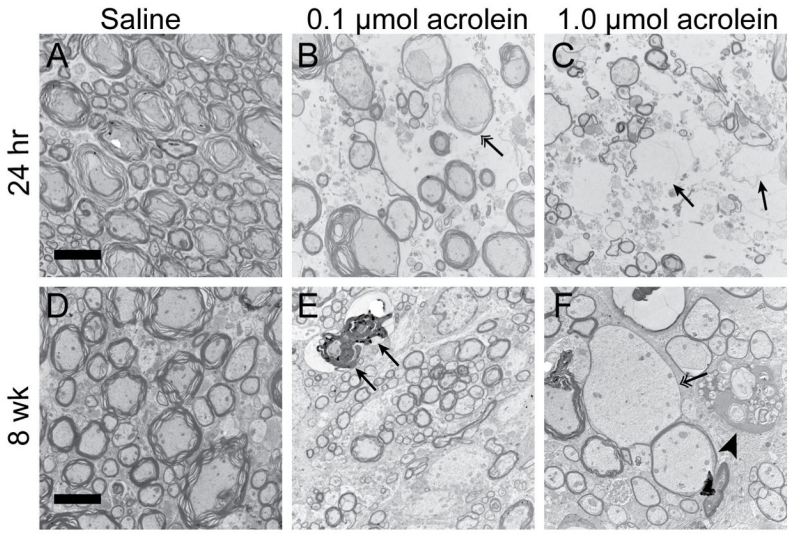

Figure 7.

Electron micrographs after acrolein injection. Representative photographs of electron microscopic images show normal appearance of axons and myelin at 24 h and 8 wk after saline injection (A, D). Low and high dose of acrolein injection, 0.1 µmol and 1.0 µmol, respectively, induced axon-myelin pathology including large axon with thin myelin (B, F, double arrows), axon degeneration (C, arrows), axon and myelin degeneration (E, arrows), and macrophage engulfment of degenerated cell debris (F, arrow head) at 24 h (A–C) and 8 wk (D–F) after acrolein injection. Bar = 6 µm.